



Title	Seasonal variations of stable carbon isotopic composition of bulk aerosol carbon from Gosan site, Jeju Island in the East China Sea
Author(s)	Kundu, Shuvashish; Kawamura, Kimitaka
Citation	Atmospheric Environment, 94, 316-322 <a href="https://doi.org/10.1016/j.atmosenv.2014.05.045">https://doi.org/10.1016/j.atmosenv.2014.05.045</a>
Issue Date	2014-09
Doc URL	<a href="http://hdl.handle.net/2115/57006">http://hdl.handle.net/2115/57006</a>
Type	article (author version)
File Information	AE94 316-322.pdf



[Instructions for use](#)

1 **Seasonal variations of stable carbon isotopic composition of bulk aerosol**  
2 **carbon from Gosan site, Jeju Island in the East China Sea**

3

4 Shuvashish Kundu<sup>a,b,\*</sup>, Kimitaka Kawamura<sup>a</sup>

5

6 <sup>a</sup>Institute of Low Temperature Science, Hokkaido University, Sapporo 060-0819, Japan

7 <sup>b</sup>Graduate School of Environmental Science, Hokkaido University, Sapporo 060-0810, Japan

8

9 \*Corresponding author phone: +1-906-231-5570; fax: +1-319-335-1270; e-mail:

10 [skundu@pop.lowtem.hokudai.ac.jp](mailto:skundu@pop.lowtem.hokudai.ac.jp); [shuvashish-kundu@uiowa.edu](mailto:shuvashish-kundu@uiowa.edu)

11

12

13

14

15

16

17

18

19

20

21

22

23

24

25

## 26 **Abstract**

27  
28         This study explores the usefulness of stable isotopic composition ( $\delta^{13}\text{C}$ ) along with  
29 other chemical tracers and air mass trajectory to identify the primary and secondary sources  
30 of carbonaceous aerosols. Aerosol samples ( $n = 84$ ) were collected continuously from April  
31 2003 to April 2004 at Gosan site in Jeju Island, South Korea. The concentrations of total  
32 carbon (TC), HCl fumed carbonate-free total carbon (fumed-TC) and their  $\delta^{13}\text{C}$  were  
33 measured online using elemental analyzer interfaced to isotope ratio mass spectrometer (EA-  
34 IRMS). Similar concentrations of TC and fumed-TC and their similar  $\delta^{13}\text{C}$  values suggest the  
35 insignificant contribution of inorganic carbon to Gosan aerosols. The monthly averaged  
36  $\delta^{13}\text{C}_{\text{TC}}$  showed the lowest in April/May (-24.2 to -24.4‰), which is related with the highest  
37 concentrations of oxalic acid (a secondary tracer). The result indicates an enhanced  
38 contribution of TC from secondary sources. The monthly averaged  $\delta^{13}\text{C}_{\text{TC}}$  in July/August (-  
39 23.0 to -22.5‰) were similar to those in January/February (-23.1‰ to -22.7‰). However,  
40 chemical tracers and air mass transport pattern suggest that the pollution source regions in  
41 January/February are completely different from those in July/August. Higher  $\delta^{13}\text{C}$  values in  
42 July/August are aligned with higher concentration ratios of marine tracers (azelaic acid/TC  
43 and methanesulfonate/TC), suggesting an enhanced contribution of marine organic matter to  
44 the aerosol loading. Higher  $\delta^{13}\text{C}$  values in January/February are associated with higher  
45 concentrations of phthalic acid and  $\text{K}^+/\text{TC}$ , indicating more contributions of carbonaceous  
46 aerosols from fossil fuel and  $\text{C}_4$ -plant biomass combustion. This study demonstrates that  
47  $\delta^{13}\text{C}_{\text{TC}}$ , along with other chemical tracers and air mass trajectory, can be used as a tracer to  
48 understand the importance of primary versus secondary pollution sources of carbonaceous  
49 aerosols in the atmosphere.

50

51 Keywords: Marine aerosol; Air pollution; Organic aerosol;  $\delta^{13}\text{C}$ ; Isotopic enrichment; Gosan  
52

## 53 **1. Introduction**

54 Atmospheric particulate matter (PM) affects the earth's radiative balance by absorbing  
55 and scattering solar radiation (direct aerosol effect) (McCormick and Ludwig, 1967;  
56 Ramanathan et al., 2001) and acting as cloud condensation nuclei (CCN) (indirect aerosol  
57 effect) (Roberts et al., 2003; Twomey, 1974). They also indirectly affect the radiative balance  
58 by changing land and ocean biogeochemical cycles through physical forcing or by adding  
59 nutrients (Mahowald, 2011). The studies on extreme air pollution episode and  
60 epidemiological and toxicological studies, have shown the relations between PM mass  
61 concentrations and increased human mortality and morbidity (Pope and Dockery, 2006). The  
62 climate and health effects largely depend upon the chemical composition of atmospheric  
63 aerosols. It is therefore very important to understand the chemical composition and pollution  
64 sources of atmospheric aerosols to formulate effective control strategies.

65 The  $\delta^{13}\text{C}$  of total carbon ( $\delta^{13}\text{C}_{\text{TC}}$ ) has been successfully used to identify and apportion  
66 the pollution sources in different parts of world (Agnihotri et al., 2011; Cachier et al., 1985;  
67 Cao et al., 2011; Chesselet et al., 1981; Jung and Kawamura, 2011; Kawamura et al., 2004;  
68 Kirillova et al., 2013; Kundu et al., 2010a; Martinelli et al., 2002; Miyazaki et al., 2010;  
69 Narukawa et al., 2008; Turekian et al., 2003; Widory et al., 2004). All of these studies used  
70 the  $\delta^{13}\text{C}_{\text{TC}}$  for understanding the primary pollution sources of carbonaceous aerosols.  
71 Secondary organic aerosols, generated in the atmosphere, can account for more than 50% of  
72 atmospheric aerosols (Cabada et al., 2004). It is therefore important to understand whether  
73  $\delta^{13}\text{C}_{\text{TC}}$  can be used to understand the primary versus secondary pollution sources of  
74 carbonaceous aerosols in the atmosphere.

75           Although there are some differences in the  $\delta^{13}\text{C}_{\text{TC}}$  in aerosols emitted from various  
76 pollution sources, the  $\delta^{13}\text{C}_{\text{TC}}$  values of particles significantly overlap among the pollution  
77 sources. The  $\delta^{13}\text{C}_{\text{TC}}$  values of coal combustion-particles are -24.4 to -23.4‰, which are  
78 similar to those of gasoline combustion-derived particles ( $-24.3 \pm 0.6\text{‰}$ ) (Widory et al.,  
79 2004). The  $\delta^{13}\text{C}_{\text{TC}}$  values of particles derived from the combustion of diesel and fuel oil are -  
80  $26 \pm 0.5\text{‰}$ , which are different than those of particles from the combustion of coal and  
81 gasoline. However, the  $\delta^{13}\text{C}_{\text{TC}}$  values of fossil fuel combustion-derived particles fall in the  
82 range of -20 to -37‰, which are  $\delta^{13}\text{C}_{\text{TC}}$  values of particles emitted from  $\text{C}_3$  plants (Das et al.,  
83 2010; Jung and Kawamura, 2011; Kohn, 2010; Turekian et al., 1998). The  $\delta^{13}\text{C}_{\text{TC}}$  values of  
84 biogenic- and anthropogenic- secondary organic aerosols (SOA) also overlap the  $\delta^{13}\text{C}_{\text{TC}}$  of  
85 particles from  $\text{C}_3$  plant. For example, the  $\delta^{13}\text{C}_{\text{TC}}$  of  $\beta$ -pinene ozonolysis-SOA has been  
86 reported to be  $-29.6 \pm 0.2\text{‰}$  whereas the  $\delta^{13}\text{C}_{\text{TC}}$  of toluene irradiation-SOA has been reported  
87 to be  $-32.5 \pm 0.3\text{‰}$  (Fisseha et al., 2009; Irei et al., 2006; Irei et al., 2011). The  $\delta^{13}\text{C}_{\text{TC}}$  values  
88 of  $\text{C}_4$  plants-derived particles are -8 to -18‰ (Das et al., 2010; Turekian et al., 1998) whereas  
89 those of marine-derived particles are -20 to -22‰ (Chesselet et al., 1981; Fontugne and  
90 Duplessy, 1978; Fry et al., 1998). Due to the overlapping between the major pollution  
91 sources, it is not straightforward to delineate among the pollution sources using only the  
92  $\delta^{13}\text{C}_{\text{TC}}$ . Some previous studies used  $\delta^{13}\text{C}_{\text{TC}}$  values along with the air mass transport patterns  
93 (e.g., Cachier et al., 1985). The  $\delta^{13}\text{C}$  along with air mass transport patterns and chemical  
94 tracers are likely to provide better information about the pollution sources.

95           Here we present the seasonal variations of  $\delta^{13}\text{C}_{\text{TC}}$  in aerosol samples collected from  
96 Gosan site at Jeju Island, South Korea. Then, we interpret the observed isotopic composition  
97 and its seasonal variations based on the chemical tracers (oxalic acid, phthalic acid, azelaic  
98 acid, methanesulfonate and  $\text{K}^+$ ) and air mass transport pattern to understand the importance

99 of both the secondary and primary sources of carbonaceous aerosols. The chemical tracers  
100 used in this study have been adopted from the previous studies (Kundu et al., 2010d).

101

## 102 **2. Experiment**

103

### 104 **2.1. Site Description**

105 Gosan site is situated on a cliff (~71 m above sea level) at the western edge of Jeju  
106 Island (33°29' N, 126°16' E) (Fig. 1). It is ~100 km south of Korean Peninsula, ~500 km east  
107 of Jiangsu province or Shanghai in China, ~200 km west of Kyushu Island in Japan, and  
108 ~1000 km northeast of Taiwan. The site is covered with grasses but there are no trees. Local  
109 anthropogenic emissions are very limited at the Gosan site (Kundu et al., 2010c, d; Lee et al.,  
110 2007). Hence, Gosan site has been used as an ideal site to evaluate air pollution as a result of  
111 the outflows from East Asia (Arimoto et al., 2004; Kawamura et al., 2004).

112

### 113 **2.2. Aerosol sampling**

114 Total suspended particles (TSP) in the atmosphere were collected at Gosan site over  
115 2–7 days throughout the year from 2003 April to 2004 April. A high volume air sampler  
116 (Kimoto AS-810) and prebaked (450 °C for 6 hours) quartz fiber filter (20 × 25 cm, Pallflex  
117 2500 QAT-UP) were used to collect TSP samples (n = 84). The sampler was installed on the  
118 roof of a trailer house (~3 m above the ground). Filters were placed in clean and prebaked  
119 glass jar (150 mL) with a Teflon-lined screw cap before and after the sampling. Samples  
120 were shipped to Sapporo, Japan and then preserved in a dark freezer room at -20 °C until  
121 analysis. Field blank filters were collected every month.

122

123 **2.3. Chemical analysis**

124 A small disc (area 2.54 cm<sup>2</sup>) of each filter sample was wrapped with a cleaned tin cup  
125 using tweezers. An autosampler was used to introduce the samples into the elemental  
126 analyzer (EA; model: NA 1500 NCS, Carlo Erba Instruments). The samples are oxidized in a  
127 combustion column packed with chromium trioxide at 1020 °C in an atmosphere of pure  
128 oxygen. The derived CO<sub>2</sub> was isolated on a gas chromatograph (GC) installed within EA and  
129 then measured with a thermal conductivity detector. Aliquots of CO<sub>2</sub> gas were then  
130 introduced online into an isotope ratio mass spectrometer (ThermoQuest, Delta Plus) through  
131 a ConFlo II interface (ThermoQuest) to monitor <sup>13</sup>C/<sup>12</sup>C ratios. The carbon isotopic  
132 composition was calculated using the following standard isotopic conversion equation.

$$\delta^{13}\text{C} (\text{‰}) = \left[ \frac{(^{13}\text{C}/^{12}\text{C})_{\text{sample}}}{(^{13}\text{C}/^{12}\text{C})_{\text{standard}}} - 1 \right] \times 1000$$

133 Another aliquot of filter samples was analyzed for TC and <sup>13</sup>C/<sup>12</sup>C ratios after the  
134 HCl-fume treatment to remove carbonate carbon (e.g., CaCO<sub>3</sub>) (Kawamura et al., 2004). The  
135 TC concentration in the field blank sample was 0.7-6% of aerosol TC concentrations and the  
136 δ<sup>13</sup>C values are reported after blank correction. The replicate analyses (n=3) of aerosol  
137 samples show that the analytical errors are in the range of 0.2-0.3‰. We have compared our  
138 TC concentrations with organic carbon (OC) and elemental carbon (EC) concentrations  
139 measured by an OC/EC analyzer (Sunset Laboratory Inc., Portland, OR). It shows that  
140 monthly average contributions of OC to TC ranged from 46.5-92.4% (average 64.8%)  
141 whereas the contributions of EC to TC ranged from 7.6-30.1% (average 18.9%). Overall, the  
142 TC concentrations were 19.6% (on average) higher than the sum of OC and EC  
143 concentrations.

144 Dicarboxylic acids, including oxalic, phthalic and azelaic acids were determined  
145 using GC-FID (GC, Agilent 6980) and GC/MS (Thermoquest, Trace MS) (Kawamura et al.,

146 2010; Kundu et al., 2010d). Methanesulfonate (MSA, a secondary marine tracer),  $K^+$  (a  
147 biomass-burning tracer) were measured using a Metrohm 761 ion chromatography (IC)  
148 system (Kundu et al., 2010d). The data of dicarboxylic acids, MSA and  $K^+$  are reported  
149 elsewhere (Kundu et al., 2010d).

150

### 151 **3. Results and discussion**

#### 152 **3.1. Seasonality of total carbon (TC) and carbonate-free total carbon (fumed-TC)**

153 Fig. 2 and Table 1 show the seasonal variations in monthly averaged concentrations  
154 of TC and fumed-TC in Gosan aerosols. The seasons in this study are defined as December to  
155 February as winter, March to May as spring, June to August as summer and September to  
156 November as fall. The average concentrations of TC and fumed-TC were found to be the  
157 highest in April/May ( $6.7$  and  $7.6 \mu\text{g m}^{-3}$ ) and the lowest in July/August ( $2.0$  and  $2.2 \mu\text{g m}^{-3}$ ).  
158 The intermediate levels of concentrations were observed in the colder months  
159 (October/November:  $3.5$  and  $3.4 \mu\text{g m}^{-3}$  and January/February:  $5.0$  and  $4.8 \mu\text{g m}^{-3}$ ). Similar  
160 levels of TC and fumed-TC suggest that most of carbonaceous aerosols are composed of  
161 organic carbon and elemental carbon and the contribution of inorganic carbon is insignificant  
162 in Gosan aerosols. The concentration levels of this study are comparable with those ( $0.6$ – $16$   
163  $\mu\text{g m}^{-3}$ ) reported for aerosol samples collected from April 2001 to March 2002 at Gosan site  
164 (Kawamura et al., 2004). The contributions of TC to aerosol mass ranged from  $0.1\%$  to  
165  $16.2\%$  with an annual average of  $6.6\%$ . Higher contributions of TC to aerosol mass ( $7.3$ –  
166  $10.0\%$ ) were observed in the spring ( $7.3$ – $10.0\%$ ) and fall ( $7.8$ – $9.9\%$ , except November)  
167 months. The lowest TC contributions were recorded in summer ( $4.2$ – $6.5\%$ ) and winter ( $5.3$ –  
168  $6.0\%$ ) months.

169 Highest concentrations and contributions of TC in spring months are consistent with  
170 the facts that almost all of the air masses in spring are transported from the heavily polluted



171 regions in east China, Korea and Japan (Fig. 1) and higher photochemical activity in the East  
172 Asian atmosphere (Mauzerall et al., 2000). The lowest concentrations and contributions in  
173 July are due to the transport of clean air masses from the East China Sea and Yellow Sea  
174 (Fig. 1). Higher concentrations of TC in the colder months (autumn and winter) are  
175 associated with air mass transport from northeastern provinces of China (Fig. 1) where the  
176 emissions from coal and other fossil fuel-combustion, as well as biofuel combustion, increase  
177 significantly in cold seasons (Cao et al., 2011; Kundu et al., 2010c). Higher contribution of  
178 TC to aerosol mass in the autumn months may be associated with an enhanced emissions  
179 from agricultural straw burning (Yang et al., 2008; Wang et al., 2009).

180

### 181 **3.2. Seasonality of $\delta^{13}\text{C}$ for TC and fumed-TC**

182 The monthly averaged  $\delta^{13}\text{C}_{\text{TC}}$  ranged between -24.4‰ to -22.5‰ with the lowest  
183 value in May and the highest value in August (Fig. 3a). The  $\delta^{13}\text{C}$  values in July/August (-23.0  
184 to -22.5‰) were similar to those in the colder months (October: -23.2‰, December: -23.4‰,  
185 January: -22.7‰ and February: -23.1‰). A similar trend with  $\delta^{13}\text{C}$  values of -24.4‰ to -  
186 22.4‰ was observed for fumed-TC. No significant difference in the  $\delta^{13}\text{C}$  values was found  
187 before and after the HCl-fume treatment of filter. The result suggests that carbonate such as  
188  $\text{CaCO}_3$  from dusts was not present and/or it was reacted with  $\text{H}_2\text{SO}_4$  in the atmosphere during  
189 a long-range transport from the source regions. This is in contrast to the situation of 2001 and  
190 2002 spring, when carbonate carbon was suggested to remain in the aerosols as the  $\delta^{13}\text{C}$   
191 values of fumed-TC were lower than the  $\delta^{13}\text{C}$  values of TC particularly in the spring  
192 (Kawamura et al., 2004).

193 The lower  $\delta^{13}\text{C}$  values in April/May are involved with the higher concentrations of  
194 oxalic acid (Fig. 3b). It is well established that oxalic acid is predominantly generated in the  
195 atmosphere due to the oxidation of various organics in the gas and aqueous phase (Warneck,

196 2003; Kawamura and Yasui, 2005; Kundu et al., 2010b; Myriokefalitakis et al., 2011). The  
197 relation of lowest  $\delta^{13}\text{C}$  with oxalic acid peak may suggest an increased contribution of  
198 secondary organic aerosols to carbonaceous aerosols at Gosan site.

199 The  $\delta^{13}\text{C}$  values in April/May at Gosan site are 5.5-8.4‰ higher than those observed  
200 in SOA from the ozonolysis of  $\beta$ -pinene and from the OH oxidation of toluene (Fig. 5a). This  
201 could be interpreted by (a) dilution of secondary sources by the other primary sources having  
202 higher  $\delta^{13}\text{C}$  values, and (b) enrichment of  $^{13}\text{C}$  by the isotopic fractionation due to the  
203 chemical ageing of organic aerosols during long-range atmospheric transport. Dilution of the  
204 secondary sources can be evidenced by the transport of various air masses during April/May  
205 at Gosan site (Fig. 1). Recently, a significant enrichment of  $^{13}\text{C}$  in remaining oxalic acid has  
206 been demonstrated during the photolysis of oxalic acid under aqueous phase in the presence  
207 of  $\text{Fe}^{3+}/\text{Fe}^{2+}$  (Pavuluri and Kawamura, 2012).

208 The concentrations of azelaic acid, methanesulfonate and  $\text{K}^+$  were normalized to  
209 better understand the role of oceanic and biomass burning emissions in driving the seasonal  
210 variations of  $\delta^{13}\text{C}$ . Higher  $\delta^{13}\text{C}$  values in summer are related with the higher concentration  
211 ratios of methanesulfonate/TC and azelaic acid/TC (Fig. 4a,b). Azelaic acid and  
212 methanesulfonate are oxidation products of oleic acid and dimethylsulfide, respectively,  
213 which are emitted from the oceans (Karl et al., 2007; Kawamura and Gagosian, 1987). The  
214 association of higher  $\delta^{13}\text{C}$  with higher ratios of methanesulfonate/TC and azelaic acid/TC  
215 suggests an increased contribution of sea spray to carbonaceous aerosols. Marine-derived  
216 carbonaceous particles are enriched with  $^{13}\text{C}$  in comparison to particles resulting from  
217 vehicular emissions,  $\text{C}_3$  plants and secondary sources (Fig. 5a).  $\text{K}^+$ /TC ratios in summer were  
218 also observed to be higher than those in May and September. The result indicates higher  
219 contribution from biomass burning of  $\text{C}_4$  plants such as wheat, rice and corn straws which is

220 associated with the burning crop residue by the end of harvest period and air mass transport  
221 from polluted East China Sea and Yellow Sea.

222 The  $\delta^{13}\text{C}$  values in colder months are similar to those in July/August (Fig. 3).  
223 However, the trajectory analysis shows that pollution sources in the colder months are  
224 different than the pollution sources in July/August at Gosan site (Fig. 1). The higher  $\delta^{13}\text{C}$   
225 values in the colder months are linked with the higher concentrations of phthalic acid (Fig.  
226 3c). Phthalic acid is either generated in the atmosphere by the oxidation of aromatic  
227 hydrocarbons emitted from fossil fuel combustion or emitted primarily from fossil fuel  
228 combustion (Fraser et al., 2003; Kawamura and Kaplan, 1987). Thus the higher  $\delta^{13}\text{C}$  values  
229 in cold seasons can be interpreted by an enhanced contribution from coal and gasoline  
230 burning. Particles produced by the combustion of coal and gasoline are generally more  
231 enriched in  $^{13}\text{C}$  than other sources such as diesel and fuel oil, SOA and  $\text{C}_3$ -plant derived  
232 particles (Fig. 5a). Large quantities of coal are burned for residential heating in north China  
233 during November to March (Cao et al., 2011). Air mass transport patterns also suggest that  
234 most of the air masses in cold seasons are transported to Gosan site from northeast China  
235 (Fig. 1).

236 Higher  $\delta^{13}\text{C}$  values in the cold seasons are also associated with higher concentration  
237 ratio of  $\text{K}^+/\text{TC}$  (Fig. 4c), suggesting an enhanced contribution from biomass burning of  $\text{C}_4$   
238 plants such as wheat, rice and corn straws. Biomass combustion has been legally prohibited  
239 in urban areas of China since 1998 (Cao et al., 2011). China has large rural population living  
240 in the village and straws are not a high-demand fuel. Hence during and after the harvest  
241 season, farmers often burn crop straws in the field as a convenient and inexpensive way to  
242 dispose agricultural waste to advance crop rotation (Yang et al., 2008; Wang et al., 2009; Fu  
243 et al., 2012). In addition, straws are also used for domestic heating during cold seasons and  
244 for cooking fuels in the rural areas throughout the year.

245

### 246 **3.3. Identification of the source regions using $\delta^{13}\text{C}$ of total carbon (TC)**

247         The comparison of  $\delta^{13}\text{C}_{\text{TC}}$  in aerosols between source regions and receptor site will  
248 provide important information about the sources and source regions. This approach may also  
249 present information on potential isotopic fractionation due to the evolution of organic  
250 aerosols as a result of chemical and physical processes. The major pollution sources at Gosan  
251 site are east China, Korea and Japan in spring, the East China Sea/Yellow Sea in summer,  
252 and northeastern China in fall and winter (Fig. 1). Figs. 5b,c compare the  $\delta^{13}\text{C}_{\text{TC}}$  in aerosols  
253 between Gosan site and source regions suggested by air mass trajectory analysis.

254         The  $\delta^{13}\text{C}_{\text{TC}}$  of atmospheric aerosols in spring in China are not available in the  
255 literature. It can be assumed that the  $\delta^{13}\text{C}_{\text{TC}}$  in spring will have similar values of summer  
256 aerosols as a result of higher contributions of SOA. The average  $\delta^{13}\text{C}_{\text{TC}}$  in summer aerosols  
257 collected in 2003 was reported to be -26.4‰ in north China and -25.9‰ in south China (Cao  
258 et al., 2011). The average  $\delta^{13}\text{C}_{\text{TC}}$  in spring aerosols at Gosan is -24.1‰, which is about 2‰  
259 higher than the  $\delta^{13}\text{C}_{\text{TC}}$  in summer aerosols in China (Figs. 5b,c). Similarly, the average  
260  $\delta^{13}\text{C}_{\text{TC}}$  in winter aerosols at Gosan site is 1.5‰ higher than those found in north China  
261 atmospheric aerosols collected in 2003 winter (Figs. 5b,c). Higher  $\delta^{13}\text{C}_{\text{TC}}$  at Gosan than the  
262 source regions may be explained by  $^{13}\text{C}$  enrichment during the long-range transport by  
263 physical/chemical evolution of organic aerosols and/or mixture of various air masses from  
264 China having different  $\delta^{13}\text{C}$  signatures. The average  $\delta^{13}\text{C}_{\text{TC}}$  in summer aerosols at Gosan is  
265 >3‰ higher than those observed in summer aerosols in north and south China (Figs. 5b,c),  
266 further confirming the marine contributions to carbonaceous aerosol. The  $\delta^{13}\text{C}_{\text{TC}}$  of marine  
267 aerosols collected during the season of higher biological activity (HBA) has been reported to  
268 be higher than those of marine aerosols collected during lower biological activity (LBA) in

269 the western Pacific Ocean (Miyazaki et al., 2010). The  $\delta^{13}\text{C}_{\text{TC}}$  has also been observed to  
270 increase in the continental aerosols when air masses were transported from the oceans  
271 (Cachier et al., 1996; Narukawa et al., 2008; Cao et al., 2013).

272

#### 273 **4. Conclusions**

274 We found that total carbon (TC) in atmospheric aerosols collected from Golan site,  
275 Jeju Island is mainly composed of organic carbon and elemental carbon with negligible  
276 amount of inorganic carbon. Inorganic carbon was insignificant even in spring when Asian  
277 dusts emitted from arid regions in China and Mongolia are often transported over the  
278 sampling site, indicating that Asian dusts may have been titrated by acids such as sulfuric  
279 acid in aerosols during a long-range atmospheric transport. Significant seasonal variations of  
280 the  $\delta^{13}\text{C}$  of both TC and fumed-TC were found in Gosan aerosols with larger values in  
281 July/August and January/February and smaller values in April/May. Seasonal variations were  
282 interpreted by the differences in pollution sources, source regions and secondary formation of  
283 organic aerosols in the atmosphere. Since the  $\delta^{13}\text{C}$  values of TC are overlapping between the  
284 pollution sources in the atmosphere, it is risky to solely depend on  $\delta^{13}\text{C}$  to identify the  
285 pollution sources. The overlapping issue was dealt in this study with the considerations of the  
286 air mass transport patterns and secondary chemical tracers including oxalic, azelaic, and  
287 phthalic acids, methanesulfonate and  $\text{K}^+$ . This study demonstrates that  $\delta^{13}\text{C}_{\text{TC}}$ , along with  
288 chemical tracers and air mass trajectory, can be used as a tracer to understand the importance  
289 of primary versus secondary sources of carbonaceous pollution. This study also shows the  
290 possible isotopic enrichment of TC in aerosols by 1.5-3‰ during a long-range transport of  
291 atmospheric aerosols from the source regions to Gosan site.

292

#### 293 **Acknowledgements**

294           This study was partly funded by the Japanese Ministry of Education, Science, Sport  
295   and Culture (MEXT) (Grant-in-Aid No. 1920405) and the Environment Research and  
296   Technology Development Fund of the Ministry of Environment (B903), Japan. S. K.  
297   appreciates the fellowship provided by the MEXT. We also thank Meehye Lee for her help in  
298   collecting aerosol samples. The authors acknowledge the NOAA Air Resources Laboratory  
299   (ARL) for giving access to the registered version of windows-based HYSPLIT model.  
300

301 **References**

- 302 Agnihotri, R., Mandal, T.K., Karapurkar, S.G., Naja, M., Gadi, R., Ahammed, Y.N.,  
303 Kumar, A., Saud, T., Saxena, M., 2011. Stable carbon and nitrogen isotopic composition  
304 of bulk aerosols over India and northern Indian Ocean. *Atmospheric Environment* 45,  
305 2828-2835.
- 306 Arimoto, R., Zhang, X.Y., Huebert, B.J., Kang, C.H., Savoie, D.L., Prospero, J.M., Sage,  
307 S.K., Schloesslin, C.A., Khaing, H.M., Oh, S.N., 2004. Chemical composition of  
308 atmospheric aerosols from Zhenbeitai, China, and Gosan, South Korea, during ACE-Asia.  
309 *J Geophys Res-Atmos* 109, doi: 10.1029/2003jd004323.
- 310 Cabada, J.C., Pandis, S.N., Subramanian, R., Robinson, A.L., Polidori, A., Turpin, B., 2004.  
311 Estimating the secondary organic aerosol contribution to PM<sub>2.5</sub> using the EC tracer  
312 method. *Aerosol Science and Technology* 38, 140-155.
- 313 Cachier, H., Buat-Menard, P., Fontugne, M., 1985. Source terms and source strengths of the  
314 carbonaceous aerosol in the tropics. *Journal of Atmospheric Chemistry* 3, 469-489.
- 315 Cao, J.J., Chow, J.C., Tao, J., Lee, S.C., Watson, J.G., Ho, K.F., Wang, G.H., Zhu, C.S., Han,  
316 Y.M., 2011. Stable carbon isotopes in aerosols from Chinese cities: Influence of fossil  
317 fuels. *Atmospheric Environment* 45, 1359-1363.
- 318 Cao J.J., , Zhu C.S., Tie X.X., Geng, F.-H., Xu, H.-M., Ho, S. S. H., Wang, G.-H., Han, Y.-  
319 M., Ho, K. -F., 2013. Characteristics and sources of carbonaceous aerosols from Shanghai,  
320 China. *Atmospheric Chemistry and Physics* 13, 803-817.
- 321 Chesselet, R., Fontugne, M., Buatmenard, P., Ezat, U., Lambert, C.E., 1981. The origin of  
322 particulate organic-Carbon in the marine atmosphere as indicated by its stable carbon  
323 isotopic composition. *Geophys Res Lett* 8, 345-348.
- 324 Das, O., Wang, Y., Hsieh, Y.P., 2010. Chemical and carbon isotopic characteristics of ash  
325 and smoke derived from burning of C-3 and C-4 grasses. *Organic Geochemistry* 41, 263-  
326 269.
- 327 Fisseha, R., Spahn, H., Wegener, R., Hohaus, T., Brasse, G., Wissel, H., Tillmann, R.,  
328 Wahner, A., Koppmann, R., Kiendler-Scharr, A., 2009. Stable carbon isotope composition  
329 of secondary organic aerosol from beta-pinene oxidation. *J Geophys Res-Atmos* 114, doi:  
330 10.1029/2008jd011326..
- 331 Fontugne, M., Duplessy, J.C., 1978. Carbon isotope ratio of marine plankton related to  
332 surface-water masses. *Earth Planet Sc Lett* 41, 365-371.
- 333 Fraser, M.P., Cass, G.R., Simoneit, B.R.T., 2003. Air quality model evaluation data for  
334 organics. 6. C-3-C-24 organic acids. *Environmental Science & Technology* 37, 446-453.
- 335 Fry, B., Hopkinson, C.S., Nolin, A., Wainright, S.C., 1998. C-13/C-12 composition of marine  
336 dissolved organic carbon. *Chem Geol* 152, 113-118.
- 337 Fu, P.Q., Kawamura, K., Chen, J., Li, J., Sun, Y.L., Liu, Y., Tachibana, E., Aggarwal, S.G.,  
338 Okuzawa, K., Tanimoto, H., Kanaya, Y., Wang, Z.F., 2012. Diurnal variations of organic  
339 molecular tracers and stable carbon isotopic composition in atmospheric aerosols over Mt.  
340 Tai in the North China Plain: an influence of biomass burning. *Atmos Chem Phys* 12,  
341 8359-8375.
- 342 Irei, S., Huang, L., Collin, F., Zhang, W., Hastie, D., Rudolph, J., 2006. Flow reactor studies  
343 of the stable carbon isotope composition of secondary particulate organic matter generated  
344 by OH-radical-induced reactions of toluene. *Atmospheric Environment* 40, 5858-5867.
- 345 Irei, S., Rudolph, J., Huang, L., Auld, J., Hastie, D., 2011. Stable carbon isotope ratio of  
346 secondary particulate organic matter formed by photooxidation of toluene in indoor smog  
347 chamber. *Atmospheric Environment* 45, 856-862.

348 Jung, J., Kawamura, K., 2011. Springtime carbon emission episodes at the Gosan background  
349 site revealed by total carbon, stable carbon isotopic composition, and thermal  
350 characteristics of carbonaceous particles. *Atmos Chem Phys* 11, 10911-10928.

351 Karl, M., Gross, A., Leck, C., Pirjola, L., 2007. Intercomparison of dimethylsulfide oxidation  
352 mechanisms for the marine boundary layer: Gaseous and particulate sulfur constituents. *J*  
353 *Geophys Res-Atmos* 112, doi: 10.1029/2006jd007914.

354 Kawamura, K., Gagosian, R.B., 1987. Implications of  $\omega$ -Oxocarboxylic Acids in the Remote  
355 Marine Atmosphere for Photooxidation of Unsaturated Fatty-Acids. *Nature* 325, 330-332.

356 Kawamura, K., Kaplan, I.R., 1987. Motor exhaust emissions as a primary source for  
357 dicarboxylic-acids in Los-Angeles ambient air. *Environmental Science & Technology* 21,  
358 105-110.

359 Kawamura, K., Kasukabe, H., Barrie, L.A., 2010. Secondary formation of water-soluble  
360 organic acids and alpha-dicarbonyls and their contributions to total carbon and water-  
361 soluble organic carbon: Photochemical aging of organic aerosols in the Arctic spring. *J*  
362 *Geophys Res-Atmos* 115, doi: 10.1029/2010jd014299.

363 Kawamura, K., Kobayashi, M., Tsubonuma, N., Mochida, M., Watanabe, T., Lee, M., 2004.  
364 Organic and inorganic composition of marine aerosols from East Asia: Seasonal variations  
365 of water-soluble dicarboxylic acids, major ions, total carbon and nitrogen, and stable C  
366 and N isotopic composition. in *Geochemical Investigations in Earth and Space Science: A*  
367 *Tribute to Isaac R. Kaplan*, edited by R. J. Hill, et al., Geochemical Society, St. Louis, MO  
368 243-265.

369 Kawamura, K., Yasui, O., 2005. Diurnal changes in the distribution of dicarboxylic acids,  
370 ketocarboxylic acids and dicarbonyls in the urban Tokyo atmosphere. *Atmospheric*  
371 *Environment* 39, 1945-1960.

372 Kirillova, E.N., Andersson, A., Sheesley, R.J., Krusa, M., Praveen, P.S., Budhavant, K.,  
373 Safai, P.D., Rao, P.S.P., Gustafsson, O., 2013.  $^{13}\text{C}$ - and  $^{14}\text{C}$ -based study of sources and  
374 atmospheric processing of water-soluble organic carbon (WSOC) in South Asian aerosols  
375 *Journal of Geophysical Research – Atmospheres*, doi: 10.1002/jgrd.50130.

376 Kohn, M.J., 2010. Carbon isotope compositions of terrestrial C3 plants as indicators of  
377 (paleo)ecology and (paleo)climate. *P Natl Acad Sci USA* 107, 19691-19695.

378 Kundu, S., Kawamura, K., Andreae, T.W., Hoffer, A., Andreae, M.O., 2010a. Diurnal  
379 variation in the water-soluble inorganic ions, organic carbon and isotopic compositions of  
380 total carbon and nitrogen in biomass burning aerosols from the LBA-SMOCC campaign in  
381 Rondonia, Brazil. *Journal of Aerosol Science* 41, 118-133.

382 Kundu, S., Kawamura, K., Andreae, T.W., Hoffer, A., Andreae, M.O., 2010b. Molecular  
383 distributions of dicarboxylic acids, ketocarboxylic acids and  $\alpha,\omega$ -dicarbonyls in biomass  
384 burning aerosols: implications for photochemical production and degradation in smoke  
385 layers. *Atmos. Chem. Phys.* 10, 2209-2225.

386 Kundu, S., Kawamura, K., Lee, M., 2010c. Seasonal variation of the concentrations of  
387 nitrogenous species and their nitrogen isotopic ratios in aerosols at Gosan, Jeju Island:  
388 Implications for atmospheric processing and source changes of aerosols. *J Geophys Res-*  
389 *Atmos* 115, doi: 10.1029/2009jd013323.

390 Kundu, S., Kawamura, K., Lee, M., 2010d. Seasonal variations of diacids, ketoacids, and  
391 alpha-dicarbonyls in aerosols at Gosan, Jeju Island, South Korea: Implications for sources,  
392 formation, and degradation during long-range transport. *J Geophys Res-Atmos* 115, doi:.

393 Lee, M., Song, M., Moon, K.J., Han, J.S., Lee, G., Kim, K.R., 2007. Origins and chemical  
394 characteristics of fine aerosols during the northeastern Asia regional experiment  
395 (atmospheric brown cloud east Asia regional experiment 2005). *J Geophys Res-Atmos*  
396 112.



397 Mahowald, N., 2011. Aerosol Indirect Effect on Biogeochemical Cycles and Climate.  
398 Science 334, 794-796.

399 Martinelli, L.A., Camargo, P.B., Lara, L.B.L.S., Victoria, R.L., Artaxo, P., 2002. Stable  
400 carbon and nitrogen isotopic composition of bulk aerosol particles in a C<sub>4</sub> plant landscape  
401 of southeast Brazil. Atmospheric Environment 36, 2427-2432.

402 Mauzerall, D.L., Narita, D., Akimoto, H., Horowitz, L., Walters, S., Hauglustaine, D.A.,  
403 Brasseur, G., 2000. Seasonal characteristics of tropospheric ozone production and mixing  
404 ratios over East Asia: A global three-dimensional chemical transport model analysis. J  
405 Geophys Res-Atmos 105, 17895-17910.

406 McCormic, R.A., Ludwig, J.H., 1967. Climate modification by atmospheric aerosols. Science  
407 156, 1358-1359.

408 Miyazaki, Y., Kawamura, K., Sawano, M., 2010. Size distributions of organic nitrogen and  
409 carbon in remote marine aerosols: Evidence of marine biological origin based on their  
410 isotopic ratios. Geophys Res Lett 37, Doi 10.1029/2010gl042483.

411 Myriokefalitakis, S., Tsigaridis, K., Mihalopoulos, N., Sciare, J., Nenes, A., Kawamura, K.,  
412 Segers, A., Kanakidou, M., 2011. In-cloud oxalate formation in the global troposphere: a  
413 3-D modeling study. Atmospheric Chemistry and Physics, 11, 5761-5782.

414 Narukawa, M., Kawamura, K., Li, S.M., Bottenheim, J.W., 2008. Stable carbon isotopic  
415 ratios and ionic composition of the high-Arctic aerosols: An increase in  $\delta^{13}\text{C}$  values from  
416 winter to spring. J Geophys Res-Atmos 113, doi: 10.1029/2007jd008755.

417 Pavuluri, C.M., Kawamura, K., 2012. Evidence for <sup>13</sup>-carbon enrichment in oxalic acid via  
418 iron catalyzed photolysis in aqueous phase. Geophys Res Lett 39.

419 Pope, C.A., III, Dockery, D.W., 2006. Health Effects of Fine Particulate Air Pollution: Lines  
420 that Connect. J Air Waste Manage 56, 709-742.

421 Ramanathan, V., Crutzen, P.J., Lelieveld, J., Mitra, A.P., Althausen, D., Anderson, J.,  
422 Andreae, M.O., Cantrell, W., Cass, G.R., Chung, C.E., Clarke, A.D., Coakley, J.A.,  
423 Collins, W.D., Conant, W.C., Dulac, F., Heintzenberg, J., Heymsfield, A.J., Holben, B.,  
424 Howell, S., Hudson, J., Jayaraman, A., Kiehl, J.T., Krishnamurti, T.N., Lubin, D.,  
425 McFarquhar, G., Novakov, T., Ogren, J.A., Podgorny, I.A., Prather, K., Priestley, K.,  
426 Prospero, J.M., Quinn, P.K., Rajeev, K., Rasch, P., Rupert, S., Sadourny, R., Satheesh,  
427 S.K., Shaw, G.E., Sheridan, P., Valero, F.P.J., 2001. Indian Ocean Experiment: An  
428 integrated analysis of the climate forcing and effects of the great Indo-Asian haze. J  
429 Geophys Res-Atmos 106, 28371-28398.

430 Roberts, G.C., Nenes, A., Seinfeld, J.H., Andreae, M.O., 2003. Impact of biomass burning on  
431 cloud properties in the Amazon Basin. J Geophys Res-Atmos 108, 4062.

432 Turekian, V.C., Macko, S., Ballentine, D., Swap, R.J., Garstang, M., 1998. Causes of bulk  
433 carbon and nitrogen isotopic fractionations in the products of vegetation burns: laboratory  
434 studies. Chem Geol 152, 181-192.

435 Turekian, V.C., Macko, S.A., Keene, W.C., 2003. Concentrations, isotopic compositions, and  
436 sources of size-resolved, particulate organic carbon and oxalate in near-surface marine air  
437 at Bermuda during spring. J Geophys Res-Atmos 108, doi: 10.1016/S0009-  
438 2541(98)00105-3.

439 Twomey, S., 1974. Pollution and the planetary albedo. Atmospheric Environment (1967) 8,  
440 1251-1256.

441 Wang, G.H., Kawamura, K., Xie, M.J., Hu, S.Y., Cao, J.J., An, Z.S., Weston, J.G., Chow,  
442 J.C., 2009. Organic molecular compositions and size distributions of chinese summer and  
443 autumn aerosols from Nanjing: characteristic haze Event caused by wheat straw burning.  
444 Environmental Science & Technology 43, 6493-6499.

445 Warneck, P., 2003. In-cloud chemistry opens pathway to the formation of oxalic acid in the  
446 marine atmosphere. Atmospheric Environment 37, 2423-2427.

447 Widory, D., Roy, S., Le Moullec, Y., Goupil, G., Cocherie, A., Guerrot, C., 2004. The origin  
448 of atmospheric particles in Paris: a view through carbon and lead isotopes. *Atmospheric*  
449 *Environment* 38, 953-961.

450 Yang, S., He, H., Lu, S., Chen, D., Zhu, J., 2008. Quantification of crop residue burning in  
451 the field and its influence on ambient air quality in Suqian, China. *Atmospheric*  
452 *Environment*, 42, 1961-1969.

453

454

455

456

457

458

459

460

461

462

463

464

465

466

467

468

469

470

471

472

473

**Table 1.** Monthly averaged stable carbon isotope ratios of bulk carbon in atmospheric aerosol samples collected from Gosan site, Jeju Island.

474

Date	Number of samples	$\delta^{13}\text{C}$ (‰)	
		<sup>a</sup> TC	<sup>b</sup> fumed-TC
January	8	-22.7	-22.6
February	8	-23.1	-22.6
March	10	-22.8	-22.7
April	17	-24.2	-24.1
May	11	-24.4	-24.4
June	7	-23.8	-23.8
July <sup>c</sup>	1	-23.0	-22.9
August	4	-22.5	-22.4
September <sup>c</sup>	2	-22.8	-23.1
October <sup>c</sup>	2	-23.2	-23.1
November	6	-24.2	-23.8
December	8	-23.4	-23.2

475

476

477

478

479

480

<sup>a</sup>TC stands for total carbon.

481

<sup>b</sup>fumed-TC is the remaining carbon on the filter after removal of inorganic carbon by HCl.

482

<sup>c</sup>Additional aerosol samples cannot be collected on July, September and October due to the mechanical failure of the aerosol samplers.

483

484

485

486 **Figure Captions:**

487 **Fig. 1.** Map showing geographical region around Gosan site along with monthly-averaged  
488 patterns of air mass transport. Gosan site is situated in the west coast of Jeju Island, South  
489 Korea. Backward trajectories for 3-days at 500 m agl were drawn with NOAA HYSPLIT  
490 model.

491

492 **Fig. 2.** Monthly-averaged variations of the concentrations total carbon (TC) and fumed-TC in  
493 Gosan aerosols. The fumed-TC was determined after HCl fume treatment. The error bar  
494 represents one standard deviation.

495

496 **Fig. 3.** Monthly averaged variations of  $\delta^{13}\text{C}$  in Gosan aerosols along with chemical tracers. a)  
497  $\delta^{13}\text{C}_{\text{TC}}$ , and  $\delta^{13}\text{C}_{\text{fumed-TC}}$ , b) oxalic acid (secondary organic aerosols (SOA) tracer from  
498 various precursors), and c) phthalic acid (SOA tracer for the oxidation of aromatic VOC).

499

500 **Fig. 4.** Variations of the monthly averaged concentration ratios of (a) azelaic acid/TC, (b)  
501 methanesulfonate/TC and (c).  $\text{K}^+$ /TC.

502

503 **Fig. 5.** Alignment of  $\delta^{13}\text{C}_{\text{TC}}$  in Gosan atmospheric aerosols (middle panel) with the  $\delta^{13}\text{C}_{\text{TC}}$  in  
504 major source aerosols (upper panel) and in source region aerosols (lower panel). Data of  
505 source regions are adopted from <sup>a</sup>Cao et al., 2011 and <sup>b</sup>Miyazaki et al., 2010. Data of the  
506 sources are adopted from <sup>c</sup>Widory et al., 2004; <sup>d</sup>Turekian et al., 2003; <sup>e</sup>Das et al., 2010;  
507 <sup>f</sup>Jung et al., 2011; <sup>g</sup>Fisseha et al., <sup>h</sup>Irei et al., 2006; and <sup>h</sup>Irei et al., 2011.

**Figure 1**

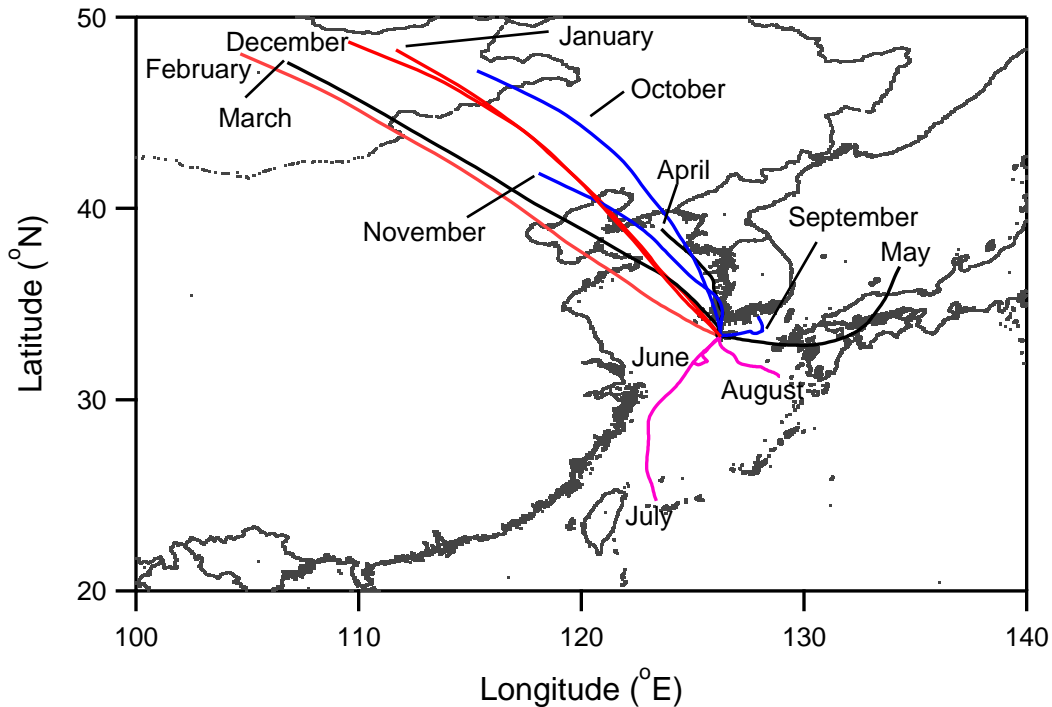


Figure 2

Figure 2.

